AIP | Applied Physics Letters

Seebeck effect in a battery-type thermocell

Wataru Kobayashi, Akemi Kinoshita, and Yutaka Moritomo

Citation: Applied Physics Letters **107**, 073906 (2015); doi: 10.1063/1.4928336
View online: http://dx.doi.org/10.1063/1.4928336
View Table of Contents: http://scitation.aip.org/content/aip/journal/apl/107/7?ver=pdfcov
Published by the AIP Publishing

Seebeck effect in a battery-type thermocell

Wataru Kobayashi,[1,a)] Akemi Kinoshita,[2] and Yutaka Moritomo[1,3]
[1]*Division of Physics, Faculty of Pure and Applied Sciences, University of Tsukuba, Ibaraki 305-8571, Japan*
[2]*Graduate School of Pure and Applied Sciences, University of Tsukuba, Ibaraki 305-8571, Japan*
[3]*Center for Integrated Research in Fundamental Science and Engineering (CiRfSE), University of Tsukuba, Ibaraki 305-8571, Japan*

(Received 16 May 2015; accepted 29 July 2015; published online 21 August 2015)

We demonstrated that battery-type thermocells, which consist of two paste-type electrodes with the same active material and electrolyte, show the Seebeck effect. The magnitudes of electrochemical Seebeck coefficient (S) of the thermocells with several layered oxides were evaluated: $-12.7\,\mu$V/K for $Na_{0.99}CoO_2$, $-29.7\,\mu$V/K for $Na_{0.52}MnO_2$, $-22.4\,\mu$V/K for $Na_{0.51}Mn_{0.5}Fe_{0.5}O_2$, and $-6.8\,\mu$V/K for $LiCoO_2$. In the thermocell with $Na_{0.99}CoO_2$, time-dependence of the electromotive force (ΔV) at a constant temperature difference (ΔT) was well reproduced by a mean-field approach of the chemical potential (ϕ)—Na^+ concentration (x) relationship, indicating that the Na^+ intercalation/deintercalation plays an intrinsic role in the electrochemical Seebeck effect. © *2015 AIP Publishing LLC*. [http://dx.doi.org/10.1063/1.4928336]

Thermoelectric (TE) technology is a fascinating technology that can convert heat into electricity and vice versa through thermoelectric phenomena in solids. The Seebeck coefficient is defined as $S \equiv \Delta V/\Delta T$, where ΔT is the temperature difference between hot and cold sides of a sample and ΔV is the induced electromotive force. Typical TE materials such as Bi_2Te_3 and PbTe exhibit high dimensionless figure-of-merit ($ZT \equiv \frac{S^2}{\rho\kappa}T$, where T, ρ, and κ represent temperature, resistivity, and thermal conductivity, respectively), and are in practical use for Peltier cooling and power generation of space vehicles.[1] However, these TE materials are expensive and include toxic and rare elements. In addition, such TE materials require high-grade heat with $T \sim 500 - 1000$ K to achieve 10%–15% of the Carnot efficiency for waste heat recovery.[2] A similar TE behavior is also observed in a thermoelectrochemical cell (thermocell) which consists of two Pt electrodes and active material such as $[Fe(CN)_6]^{3-}$/$[Fe(CN)_6]^{4-}$. The active materials are solved in water[3,4] or ionic liquid.[5–8] The temperature difference (ΔT) unbalances the redox reaction (e.g., $[Fe(CN)_6]^{3-} + e^- \leftrightarrow [Fe(CN)_6]^{4-}$) between the Pt electrodes, and causes the electromotive force (ΔV). This type of Seebeck effect is called as "electrochemical" Seebeck effect. Another example is an all-solid thermocell consists of superionic conductor and Ag/AgI electrodes. Kawamura *et al.* observed a large S of -0.5 mV/K due to ionic contribution to Seebeck coefficient in a thermocell with Ag_3SBr electrolyte.[9] Schiraldi *et al.* also measured S of a superionic glass $AgI:Ag_2O\text{-}B_2O_3$ sandwiched by Ag electrodes, and concluded that Ag^+ ion coming from AgI in the glass plays a major role in determining the properties of the glass.[10]

Here, we propose another type of thermocell (see Fig. 1), which consists of two paste-type electrodes with the same active material, instead of the expensive Pt electrodes. The configuration is the same as that of a lithium/sodium-ion secondary battery (LIB/SIB) with the exception that the same active material is used in both the anode and cathode. Hereafter, we will call the thermocell as *battery-type* thermocell. The battery-type thermocell is low-cost and easy to fabricate, because the materials and production process are the same as those of LIB/SIB. In addition, we can extract TE functionalities from insoluble active materials in the battery-type thermocell. The layered oxides Na_xMO_2 ($0.5 \le x \le 1.0$; M is a transition metal.), which can store one Na^+ per a formula unit, are prototypical active materials for SIBs.[11] As shown in Fig. 1, Na_xMO_2 consists of alternately stacked MO_2 layers and Na layers. With an increase (decrease) in temperature, the deintercalation (intercalation) process of Na^+ is activated because the number of the Na^+ configuration increases with decrease in x from 1. Then, if we apply ΔT between the two electrodes, ΔV is expected.

In this paper, we demonstrated that battery-type thermocells, which consist of two paste-type electrodes with the same active material and electrolyte, show electrochemical Seebeck effect. The magnitudes of S of the thermocells with several layered oxides were evaluated: $-12.7\,\mu$V/K for $Na_{0.99}CoO_2$, $-29.7\,\mu$V/K for $Na_{0.52}MnO_2$, $-22.4\,\mu$V/K for $Na_{0.51}Mn_{0.5}Fe_{0.5}O_2$, and $-6.8\,\mu$V/K for $LiCoO_2$. We found that $|\Delta V|$ of the thermocell under constant ΔT decreases with time (t), which is in sharp contrast with the conventional TE

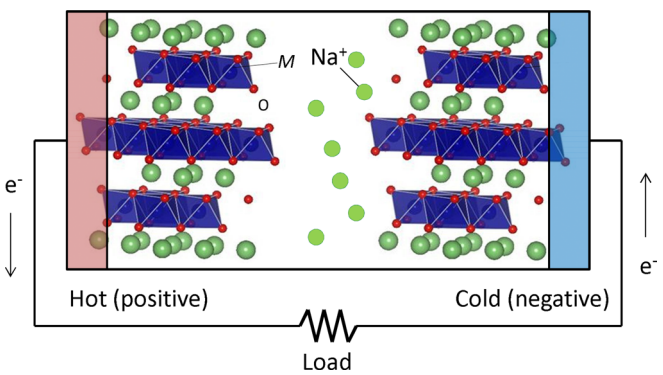

FIG. 1. Schematic figure of battery-type thermocell, which consists of two paste-type electrodes with the same active material. The active material is layered oxide (Na_xMO_2, where M is a transition metal), which can store one Na^+ per a formula unit.

a)Electronic mail: kobayashi.wataru.gf@u.tsukuba.ac.jp

materials. The behavior is quantitatively reproduced by a mean-field approach of the chemical potential [$\phi(x)$] by assuming that a part (δ) of the Na sites is active. Characteristics of the thermocell presented here are (1) it can store thermal energy as chemical energy in the electrode material and (2) it can generate ionic current under temperature difference. Such a combination of the accumulation and the generation of electricity in the thermocell can be applied under temperature variation for a battery of a sensor that requires small power.

Powders of $Na_{0.99}CoO_2$, $Na_{0.52}MnO_2$, and $Na_{0.51}Mn_{0.5}Fe_{0.5}CoO_2$ were prepared by solid state reaction. Details of the synthesis procedures were described elsewhere.[12–14] The x-ray diffraction (XRD) patterns were measured by Rigaku RINT2000PC using a monochromatic CuKα radiation. All the reflections were indexed with the P2-type structure ($P6_3/mmc$) for $Na_{0.52}MnO_2$ and $Na_{0.51}Mn_{0.5}Fe_{0.5}O_2$, and the O3-type structure ($R\bar{3}m$) for $Na_{0.99}CoO_2$. The actual Na concentration (x) in the compound was determined by the Rietveld refinement based on the synchrotron radiation powder x-ray diffraction patterns. We used paste-type electrodes of $Na_{0.99}CoO_2$, $Na_{0.52}MnO_2$, and $Na_{0.51}Mn_{0.5}Fe_{0.5}O_2$. Active material, acetylene black, and polyvinylidenefluoride (PVDF) were mixed in a ratio of 8:1:1 with N,N-dimethylformamide and pasted on Al foil with a thickness of 20 μm. The electrodes were well dried at 100 °C in vacuum. We also investigated commercialized $LiCoO_2$ electrode (Hosen Corporation).

We fabricated CR2032-type coin cell as battery-type thermocell, because the cell is free from moisture that degrades both electrode and electrolyte. The coin cell was assembled as follows: from the bottom, a stainless-steel cap (SUS316L), the first electrode, a separator with electrolyte, the second electrode, a stainless-steel mesh, three stainless-steel plates, a stainless-steel washer, and a stainless-steel cap were layered and caulked. Note that the first and second electrodes are the same. In the sodium compounds, 1 mol/l $NaClO_4$ dissolved in propylene carbonate was used as the electrolyte. In $LiCoO_2$, 1 mol/l $LiClO_4$ dissolved in ethylene carbonate/diethyl carbonate was used as the electrolyte. ΔT was induced by Peltier elements attached to the top and bottom of the thermocell and detected by two copper-constantan thermocouples. The voltage difference between the thermocouples were measured by nanovolt meter (Agilent 34420A), and converted to ΔT. ΔV was measured by electrometer (ADCMT8252). These equipments were controlled by LabVIEW program. ΔT (input) and ΔV (output) was measured against t at room temperature. We checked that ΔV of the thermocell without active material exhibits negligibly small voltage ($\sim 10^{-3}$ mV) compared with ΔV ($\sim$0.1 mV).

Figures 2(a) and 2(b) show ΔT (input) and ΔV (output) of the battery-type thermocell with $Na_{0.99}CoO_2$ against t. We input a pseudo-rectangular thermal wave (ΔT) to the thermocell through the Peltier elements. Importantly, the sign of ΔV flips in an opposite direction to ΔT. To precisely investigate the correlation between ΔT and ΔV, we replotted the data points on the $\Delta T - \Delta V$ plane [Fig. 2(c)]. We found that ΔV changes in proportion to ΔT even though the data points are scattered. The electrochemical Seebeck coefficient S ($=-12.7$ μV/K) corresponds to the gradient of the $\Delta V - \Delta T$ plot (broken line).

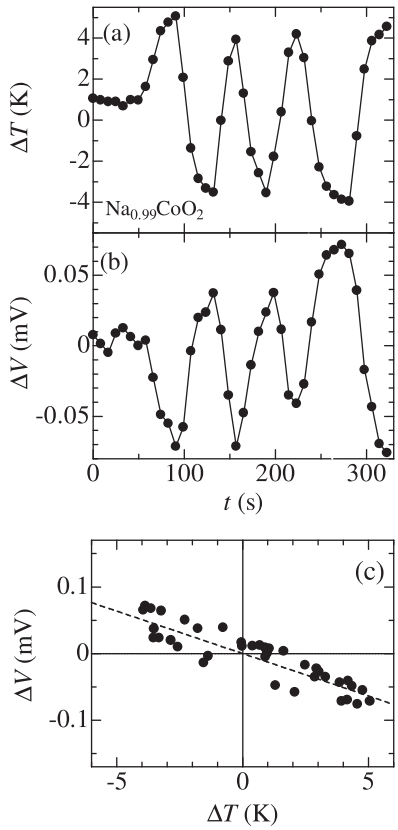

FIG. 2. Time (t) dependence of (a) ΔT and (b) ΔV of battery-type thermocell with $Na_{0.99}CoO_2$ at 298.0 K. (c) $\Delta V - \Delta T$ plot of the data. The broken line represents a least-squares fitting with a linear function.

Similar relations between ΔT (input) and ΔV (output) were observed in the other compounds. Figure 3 shows $\Delta V - \Delta T$ plots of the battery-type thermocells with $Na_{0.52}MnO_2$, $Na_{0.51}Mn_{0.5}Fe_{0.5}O_2$, and $LiCoO_2$. As indicated by least-squares fitted straight lines, the magnitudes of S were evaluated to be -29.7, -22.4, and -6.8 μV/K for the thermocells with $Na_{0.52}MnO_2$, $Na_{0.51}Mn_{0.5}Fe_{0.5}O_2$, and $LiCoO_2$, respectively. Thus determined S values were listed in Table I.

Figure 4 shows (a) ΔT and (b) ΔV of the battery-type thermocell with $Na_{0.99}CoO_2$ against t. We applied a rectangular pulse ($\Delta T \sim 22$ K) from 137 s to 634 s and from 1325 s to 1620 s by changing temperatures (T_H and T_L) of hot and cold sides of the thermocell as indicated by red and blue broken lines in Fig. 4(a). ΔV discontinuously jumps to -0.15 mV at

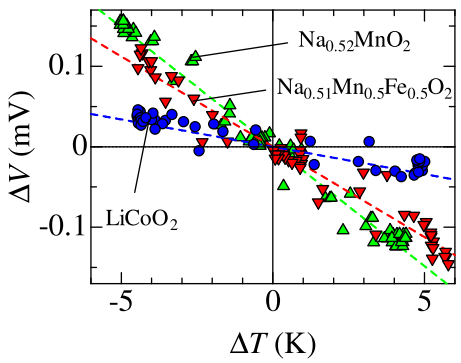

FIG. 3. $\Delta V - \Delta T$ plots of battery-type thermocells with $Na_{0.52}MnO_2$, $Na_{0.51}Mn_{0.5}Fe_{0.5}O_2$, and $LiCoO_2$ at 293.8–297.5 K. The broken lines represent least-squares fittings with a linear function.

TABLE I. Electrochemical Seebeck coefficient (S) of battery-type thermocells with layered oxide at temperature (T).

Compound	S (μV/K)	T (K)
$Na_{0.99}CoO_2$	−12.7	298.0
$Na_{0.52}MnO_2$	−29.7	293.8
$Na_{0.51}Mn_{0.5}Fe_{0.5}O_2$	−22.4	297.5
$LiCoO_2$	−6.8	294.2

1325 s, and $|\Delta V|$ gradually decreases to zero at 1600 s. Such a t-dependent behavior is not observed in the conventional TE materials. The TE negative current causes the Na^+ ion transfer from hot to cold electrodes through the electrolyte. Then, x in the hot (cold) electrode gradually decreases (increases) with t. The resultant difference in x between the two electrodes causes the battery voltage, which suppresses the thermoelectromotive force. In short, the battery-type thermocell is charged by the temperature difference. Actually, we observed positive voltage output ($\Delta V = 0.15$ mV) when we release the temperature difference at 1620 s. ΔV gradually decreases to nearly zero, which corresponds to the discharge process in the secondary battery. In the discharge process, x in the positive (negative) electrode gradually increases (decreases) with t until the x values of both the electrodes become the same.

First, let us consider the magnitude of S in terms of the x-dependence of the ionic potential [$\phi(x)$]. The layered oxides Na_xMO_2 can store one Na^+ per a formula unit. In a mean-field approximation, $\phi(x)$ is easily calculated from the number of the Na^+ configurations against x

$$\phi = \phi_0 + k_B T \ln\left(\frac{x}{1-x}\right), \tag{1}$$

where ϕ_0 and k_B represent the site potential and the Boltzmann constant, respectively. ΔV is defined by

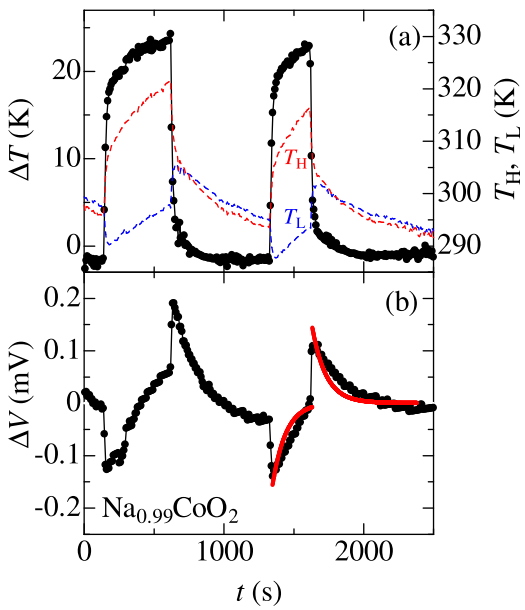

FIG. 4. Time (t) dependence of (a) ΔT and (b) ΔV of the battery-type thermocell with $Na_{0.99}CoO_2$. Red and blue broken lines in (a) represent temperatures (T_H and T_L) of hot and cold sides of the thermocell. Red curves in (b) are results of a mean-field calculation with an adjustable parameter of δ (=0.018) that represents a ratio of active sites to all the Na sites.

$\phi(x_H) - \phi(x_L)$, where x_H (x_L) is the Na^+ concentration at the hot (cold) electrode. Immediately after applying ΔT, ΔV is expressed as

$$\Delta V = -\frac{k_B}{e}\Delta T \ln\left(\frac{x}{1-x}\right), \tag{2}$$

because Na^+ transfer does not occurs (x does not change) at this stage. Then, S is easily calculated as

$$S \equiv \frac{\Delta V}{\Delta T} = -\frac{k_B}{e}\ln\left(\frac{x}{1-x}\right). \tag{3}$$

Using the formula, S is calculated to be $-395.2\,\mu$V/K at $x = 0.99$, which is one order higher than the observed value ($-12.7\,\mu$V/K; see Table I). The discrepancy is ascribed to the spatial inhomogeneity of ϕ and resultant reduction of the active Na sites (*vide infra*).

Now, let us proceed to the ΔV - t curve. Importantly, the thermally induced ΔV causes not only the electric current outside the thermocell but also the ionic current [$I(t)$] inside the thermocell. As a result, x_H (x_L) gradually decreases (increases) with t. To analyze the $\Delta V - t$ curve, we assume the Ohmic relation: $I(t) = \Delta V(t)/R$, where R is the ionic resistance. The amount [$\Delta x(t)$] of the transferred Na^+ ions is expressed as

$$\Delta x(t) = \frac{1}{mF}\int_0^t \frac{\Delta V(t)}{R}dt, \tag{4}$$

where m ($=8.78\times10^{-6}$ mol) and F represent number of moles of active material and Faraday constant, respectively. Accordingly, $x_H(t)$ [$x_L(t)$] changes as $x - \Delta x(t)$ [$x + \Delta x(t)$] with t. After a tedious calculation, we obtained the relation,

$$\Delta V(t) = -\frac{k_B}{e}\left\{T_H \ln\left(\frac{x-\Delta x(t)}{1-x+\Delta x(t)}\right) - T_L \ln\left(\frac{x+\Delta x(t)}{1-x-\Delta x(t)}\right)\right\}. \tag{5}$$

With use of the experimentally-obtained values at $t = 1500$ K, i.e., $m = 8.78 \times 10^{-6}$ mol, $T_H = 312.8$ K, $T_L = 291.1$ K, and $R = 600\ \Omega$, Eq. (5) qualitatively reproduce the several features of the $\Delta V - t$ curve, i.e., (1) discontinuous negative jump immediately after applying ΔT (≥ 0) and gradual decreases in magnitude and (2) discontinuous positive jump immediately after release of ΔT and gradual decreases in magnitude. Δx at 1620 s was evaluated to be 0.0015 from the fitting. The calculated value (=−8.6 mV), however, is two orders of magnitude higher than the observed value (=−0.15 mV). The discrepancy is partly due to the overestimation of ΔT. If we consider the thermal resistances of the stainless-steel parts of the thermocell without contact thermal resistances, the actual temperature difference is reduced to ≈40% of ΔT.

The discrepancy between the calculation and observation is probably ascribed to the spatial inhomogeneity of ϕ. The inhomogeneity of ϕ may be attributed to the surface effect, local deformation of active material, and electric connection between active material and acetylene blacks. If the spatial distribution of ϕ is much wider than ΔT, only part of

the Na sites is active and takes part in the TE phenomena. The other sites are inactive, and hence, do not contribute to the entropy change. Here, we define δ as a ratio of the active sites. Then, instead of numbers of the Na sites (N) and Na^+ ions (n), $\delta \times N$ and $\delta \times n$ are used for the entropy calculation. This modification results in a simple multiplication by a prefactor of δ in Eqs. (2), (3), and (5), and by a prefactor of $1/\delta$ in Eq. (4). By setting $\delta = 0.018$, we satisfactorily reproduce the S value and t-dependence of ΔV [Fig. 4(b)] of $Na_{0.99}CoO_2$. The S value is calculated to be $-7.1\ \mu V/K$ at $x = 0.99$, which is the same order of the observed value ($-12.7\ \mu V/K$). The red curves in Fig. 4(b) are the calculated result based on the modified Eq. (5). The calculation quantitatively reproduced the $\Delta V - t$ curve. These arguments imply that the S value of the battery-type thermocell is enhanced if we apply higher ΔT and/or fabricate a more homogeneous electrode.

In this model, contribution of electronic Seebeck effect is not taken into account. Since the battery-type thermocell consists of an electrolyte and thermoelectric materials, in principle, electronic Seebeck coefficient (S_e) can be observed. Such a contribution, however, seems negligible in the present case. In Fig. 4(b), at least, S_e should not be observed after 1620 s because ΔT is zero after 1620 s. Even in between 1325 s and 1620 s with ΔT, the data seem to obey Eq. (5) indicating that the electronic contribution is negligible. One possible reason is a small ΔT in the active material because of $\approx 20\ \mu m$ thickness of the electrode.

Finally, we discuss possible ways to further improve the thermoelectric properties of the thermocells with layered oxides. As a cathode material of SIBs, layered Na_xMO_2 is widely investigated in terms of electrochemical and structural properties.[11] According to Lei *et al.*,[15] O3-type Na_xCoO_2 continuously changes from O3 phase with $x = 1.0$ to P3′ phase with $x = 0.5$ through biphasic regions. Accordingly, V changes against x. A stable single phase exhibits a large change in V against x, while a biphasic phase exhibits a small change in V against x. Similar features are observed in P2-type Na_xCoO_2[16] and are well interpreted by a first-principle calculation.[17] This suggests that use of a layered oxide in a stable single phase is preferable to obtain a large ΔV.

Another aspect is Na^+ current that contributes a power of the thermocell. The Na^+ current in Na_xMO_2 depends on diffusion constant (D) through Fick's laws of diffusion. D is a function of activation energy (E_a). E_a is also calculated by a first-principle calculation.[18] For example, E_a of O3-type Na_xCoO_2 decreases with x. Small E_a may cause a large D. According to a first-principle calculation by Kang and Ceder,[19] E_a of $LiMO_2$ was found to highly depend on interlayer distance (d). In this calculation, smaller d causes larger potential barrier of Li^+ because of narrower interlayer space for diffusion. Similar tendency is experimentally observed by Shibata *et al.* for P2-type Na_xMO_2.[20] The small d also causes a reduction of charge-transfer resistance.[20] Thus, to generate large Na^+ current in the thermocell, Na_xMO_2 with large d is desirable. Cyclability is also an important aspect that limits operating life of the thermocell. Toward a long operating life, good cyclability is essential. O3-type Na_xCoO_2 (Ref. 12) (P2-type $Na_xMn_{0.5}Fe_{0.5}O_2$ (Ref. 14)) exhibits good cyclability, in which the capacity after 30 cycles remains 92(79) % of the initial capacity [=140(190) mAh/g]. On the other hand, P2-type Na_xMnO_2 structure gradually collapses and yields an amorphous material after the first eight cycles. This is caused by the continuous strains and distortions resulting from the insertion and extraction of Na^+ ions.[21] Thus, a layered oxide with less strains and distortions against x should be selected as an electrode.

In conclusion, we have fabricated battery-type thermocells with layered oxides and evaluated electrochemical Seebeck coefficient (S). We observe characteristic t-dependence of ΔV, i.e., (1) discontinuous negative jump immediately after applying ΔT (≥ 0) and gradual decreases to zero and (2) discontinuous positive jump immediately after release of ΔT and gradual decrease in magnitude. These behaviors are quantitatively reproduced by a mean-field approach of $\phi(x)$ assuming that part (δ) of the Na sites is active.

This work was partly supported by a research grant from the Thermal and Electric Technology, Inc., Foundation, A-STEP program from Japan Science and Technology Agency, and Grant-in-Aid for Scientific Research (23684022) from the Ministry of Education, Culture, Sports, Science and Technology (MEXT), Japan.

[1]H. J. Goldsmid, *Introduction to Thermoelectricity* (Springer-Verlag, Berlin, 2010).
[2]C. B. Vining, Nat. Mater. **8**, 83 (2009).
[3]T. I. Quickenden and Y. Mua, J. Electrochem. Soc. **142**, 3985 (1995).
[4]Y. Mua and T. I. Quickenden, J. Electrochem. Soc. **143**, 2558 (1996).
[5]D. R. MacFarlane, N. Tachikawa, M. Forsyth, J. M. Pringle, P. C. Howlett, G. D. Elliott, J. F. Davis, Jr., M. Watanabe, P. Simon, and C. A. Angell, Energy Environ. Sci. **7**, 232 (2014).
[6]T. J. Abraham, D. R. MacFarlane, and J. M. Pringle, Chem. Commun. **47**, 6260 (2011).
[7]M. Bonetti, S. Nakamae, M. Roger, and P. Guenoun, J. Chem. Phys. **134**, 114513 (2011).
[8]N. Jiao, T. J. Abraham, D. R. MacFarlane, and J. M. Pringle, J. Electrochem. Soc. **161**, D3061 (2014).
[9]J. Kawamura, M. Shimoji, and H. Hoshino, J. Phys. Soc. Jpn. **50**, 194 (1981).
[10]A. Schiraldi, E. Pezzati, and P. Baldini, J. Phys. Chem. **89**, 1528 (1985).
[11]N. Yabuuchi, K. Kubota, M. Dahbi, and S. Komaba, Chem. Rev. **114**, 11636 (2014).
[12]H. Yoshida, N. Yabuuchi, and S. Komaba, Electrochem. Commun. **34**, 60 (2013).
[13]D. Tanabe, T. Shimono, W. Kobayashi, and Y. Moritomo, Phys. Status Solidi RRL **7**, 1097 (2013).
[14]N. Yabuuchi, M. Kajiwara, J. Iwatate, H. Nishikawa, S. Hitomi, R. Usui, Y. Yamada, and S. Komaba, Nat. Mater. **11**, 512 (2012).
[15]Y. Lei, X. Li, L. Liu, and G. Ceder, Chem. Mater. **26**, 5288 (2014).
[16]R. Berthelot, D. Carlier, and C. Delmas, Nat. Mater. **10**, 74 (2011).
[17]Y. Hinuma, Y. S. Meng, and G. Ceder, Phys. Rev. B **77**, 224111 (2008).
[18]Y. Mo, S. P. Ong, and G. Ceder, Chem. Mater. **26**, 5208 (2014).
[19]K. Kang and G. Ceder, Phys. Rev. B **74**, 094105 (2006).
[20]T. Shibata, W. Kobayashi, and Y. Moritomo, Appl. Phys. Express **7**, 067101 (2014); **8**, 029202 (2015).
[21]A. Caballero, L. Hernán, J. Morales, L. Sánchez, J. Santos Peña, and M. A. G. Aranda, J. Mater. Chem. **12**, 1142 (2002).